Fluorosulfonic Acid and Chlorosulfonic Acid: Possible Candidates for OH-Stretching Overtone-Induced Photodissociation

Joseph R. Lane

Department of Chemistry, University of Otago, P.O. Box 56, Dunedin 9054, New Zealand

Henrik G. Kjaergaard*

Department of Chemistry, University of Otago, P.O. Box 56, Dunedin 9054, New Zealand, and The Lundbeck Foundation Center for Theoretical Chemistry, Department of Chemistry, Aarhus University, DK-8000, Aarhus C, Denmark

Received: June 8, 2007

We have calculated the stationary points and internal reaction coordinate pathway for the dissociation of fluorosulfonic acid (FSO_3H) and chlorosulfonic acid ($ClSO_3H$). These sulfonic acids dissociate to sulfur trioxide and hydrogen fluoride and chloride, respectively. We have calculated the frequencies and intensities of the OH-stretching transitions of FSO_3H and $ClSO_3H$ with an anharmonic oscillator local mode model. We find that excitation of the fourth and third OH-stretching overtones provide adequate energy for photodissociation of FSO_3H and $ClSO_3H$, respectively. We propose that experimental detection of the products of OH-stretching overtone-induced photodissociation of FSO_3H and $ClSO_3H$ would be easier than the sulfuric acid (H_2SO_4) equivalent. The photodissociation of H_2SO_4 is thought to be important in the stratosphere. The FSO_3H and $ClSO_3H$ experiment could be used in proxy to support the recently proposed OH-stretching overtone-induced photodissociation mechanism of H_2SO_4.

Introduction

The concentration and distribution of sulfur compounds in the stratosphere have been of increasing interest because of the important role they play in the formation of atmospheric aerosols.[1−4] In particular, the photodissociation of sulfuric acid (H_2SO_4) is thought to explain the anomalous enhancement of the polar stratospheric sulfate aerosol layer in the springtime.[3−6] Photodissociation of H_2SO_4 was initially assumed to occur via absorption of an ultra-violet photon to a dissociative electronically excited state. However, several attempts to measure the electronic absorption spectrum of H_2SO_4 were unable to identify any absorption up to 140 nm.[7,8] High level ab initio calculations suggest that the lowest-lying electronic excitation in H_2SO_4 occurs around 144 nm and that the cross section in the actinic region is very small.[9,10]

On the basis of early work by Crim,[11,12] Vaida et al. proposed that excitation of a high OH-stretching vibrational overtone in H_2SO_4 with visible photons could provide sufficient energy for photodissociation.[3] The energy required for dissociation of sulfuric acid to sulfur trioxide and water ($H_2SO_4 \rightarrow H_2O + SO_3$) has been calculated to be in the range 32−40 kcal mol^{-1} at the MP2 and B3LYP levels of theory.[13,14] The OH-stretching fundamental and overtone spectra of H_2SO_4 have been previously recorded in the vapor phase with conventional ($\Delta v_{OH} = 1-3$) and cavity ringdown ($\Delta v_{OH} = 4$ and 5) spectroscopy.[8,15,16] With an energy barrier of 32 kcal mol^{-1}, excitation of an OH-stretching transition with $\Delta v \geq 4$ (13490 cm^{-1} or 39 kcal mol^{-1}) would provide adequate energy for dissociation. The intensity of this OH-stretching transition is sufficient to account for the inferred photodissociation rate of H_2SO_4 as a source of polar stratospheric sulfate aerosol.[3]

The importance of overtone-induced photodissociation reaction mechanisms have been shown in both laboratory and field measurements for atmospheric radical production from, for example, hydrogen peroxide,[17−19] nitric acid,[20,21] peroxynitrous acid,[21−25] and hydroxymethyl hydroperoxide.[26] Theoretically, decarboxylation of organic acids have also been suggested to proceed via vibrationally excited overtones.[27] However, experimental confirmation of the OH-stretching overtone-induced photodissociation of H_2SO_4 has remained illusive. There are inherent difficulties in monitoring such an experiment, as H_2SO_4 has an extremely low vapor pressure and exists in equilbiria with H_2O and SO_3 in the gas phase. For vapor-phase spectroscopic studies, H_2SO_4 is typically generated in a gas flow cell by mixing known vapor flows of H_2O and SO_3 at elevated temperatures of 400−500 K ($H_2O + SO_3 \rightarrow H_2SO_4$).[7] This approach leads to large background signal from the H_2O and SO_3 starting materials, making it extremely difficult to measure the H_2O and SO_3 as products of photodissociation. For this reason, we suggest that the study of a closely related molecule to H_2SO_4, which does not have these same inherent difficulties, could be used by proxy to validate the OH-stretching overtone-induced photodissociation mechanism of H_2SO_4. If we subsitute one of the OH groups in H_2SO_4 with a halogen atom (X = F, Cl), we have two potential candidates: fluorosulfonic acid (FSO_3H) and chlorosulfonic acid ($ClSO_3H$). These closely related sulfonic acid derivatives are thought to have a similar dissociation reaction mechanism to H_2SO_4. FSO_3H and $ClSO_3H$ are liquids with reasonable vapor pressures. Experimental detection of HF/HCl and SO_3, as the products of OH-stretching

* To whom correspondence should be addressed. E-mail: henrik@alkali.otago.ac.nz. Fax: 64-3-479-7906. Phone: 64-3-479-5378.

10.1021/jp074436d CCC: $37.00
Published on Web 09/01/2007

overtone-induced photodissociation, should be possible as there should be no HF/HCl and SO_3 background.

Previously, the formation reactions of fluorosulfonic, chlorosulfonic, and bromosulfonic acid ($HX + SO_3 \rightarrow XSO_3H$, where X = F, Cl, Br) have been investigated theoretically with the B3LYP/6-311++G** method.[28] An anomalously high binding energy of $HF{\cdot}SO_3$ and unusual trends between the FSO_3H, $ClSO_3H$, and $BrSO_3H$ reactions were found.[28]

In this work, we investigate the dissociation reaction of FSO_3H and $ClSO_3H$ to $HF + SO_3$ and $HCl + SO_3$, respectively. We have calculated the stationary points and internal reaction coordinate pathway with a range of ab initio and density functional methods with Dunning type correlation consistent basis sets. We have also calculated the OH-stretching overtone spectra of FSO_3H and $ClSO_3H$ to assess what quanta of excitation is required for OH-stretching overtone-induced photodissociation to occur. We use a simple one-dimensional (1D) anharmonic oscillator local mode model with dipole moment functions obtained from ab initio coupled-cluster calculations.[29−35]

Theory and Calculations

We have optimized the geometries of the reactants, intermediates, and products for the dissociation of FSO_3H and $ClSO_3H$ to $HF + SO_3$ and $HCl + SO_3$, respectively. We have optimized using the HF, MP2, CCSD, and CCSD(T) ab initio theories as well as the B3LYP density functional theory. The optimization threshold criterion was set to gradient $= 1 \times 10^{-5}$ au, stepsize $= 1 \times 10^{-5}$ au, and energy $= 1 \times 10^{-7}$ au. We have used the Dunning type correlation consistent basis sets supplemented with additional tight d basis functions on the sulfur and chlorine atoms, aug-cc-pV(D+d)Z and aug-cc-pV(T+d)Z.[36] These additional tight d functions have been shown to improve the convergence of geometries and energies of compounds and weakly bound monohydrated complexes containing second row elements.[37−39]

For the complexes $HF{\cdot}SO_3$ and $HCl{\cdot}SO_3$, we have also employed a full counterpoise- (CP) corrected optimization scheme to assess the effects of basis set superposition error (BSSE) on our optimized geometry.[40] We have recently shown that this approach provides geometries of monohydrated complexes with an accuracy that is comparable to or better than most experimentally determined geometries.[38,41]

Harmonic frequency calculations were performed at the HF, B3LYP, and MP2 level of theory with the aug-cc-pV(D+d)Z and aug-cc-pV(T+d)Z basis sets and at the CCSD(T) level of theory with the aug-cc-pV(D+d)Z basis set. The optimized geometries were determined to be true minima by the absence of imaginary frequencies, while the presence of a single imaginary frequency was used to identify transition states along the reaction path. We estimate the zero-point vibrational energy (ZPVE) correction using unscaled B3LYP/AV(T+d)Z harmonic frequencies. The intrinsic reaction coordinate, which follows the minimum-energy path from the transition state, has been calculated in both directions using the HF, B3LYP, and MP2 levels of theory with the aug-cc-pV(D+d)Z and aug-cc-pV(T+d)Z basis sets to confirm the connections between the stationary points (reactants, transitions states, and complexes).

The dimensionless oscillator strength f of a transition from the vibrational ground state $|0\rangle$ to a vibrationally excited state $|\upsilon\rangle$ is given by[42,43]

$$f_{\upsilon 0} = 4.702 \times 10^{-7}[\text{cm D}^{-2}]\tilde{\nu}_{\upsilon 0}|\mu_{\upsilon 0}|^2 \qquad (1)$$

where $\tilde{\nu}_{\upsilon 0}$ is the vibrational wavenumber of the transition in cm^{-1} and $\mu_{\upsilon 0} = \langle \upsilon|\mu|0\rangle$ is the transition dipole moment matrix element in Debye (D).

We calculate the OH-stretching wavenumbers and oscillator strengths for FSO_3H and $ClSO_3H$ within the local mode model.[29] The OH-stretching vibration is considered isolated from the other vibrational modes.[31−35] The 1D Schrödinger equation is solved with two different approaches.[41] The first approach describes the OH-stretching local mode by a Morse oscillator with the vibrational energy levels given by

$$E(\upsilon)/(hc) = \left(\upsilon + \frac{1}{2}\right)\tilde{\omega} - \left(\upsilon + \frac{1}{2}\right)^2 \tilde{\omega}x \qquad (2)$$

and the associated well-known Morse oscillator wavefunctions. The Morse oscillator frequency $\tilde{\omega}$ and anharmonicity $\tilde{\omega}x$ are found from the second-, third-, and fourth-order derivatives of the potential energy curve as described previously.[35,44] These derivatives are found by fitting an eighth-order polynomial to a nine-point ab initio calculated potential energy curve, obtained by displacing the OH bond from −0.2 to 0.2 Å in 0.05 Å steps around equilibrium.[30,45]

In the second approach, the 1D Schrödinger equation is solved numerically using a finite element method to give both the vibrational energy levels and wavefunctions.[46] The potential energy curve used for this covers the range from −0.3 to 0.6 Å in 0.025 Å steps around equilibrium. This ensures converged energy levels, better than 0.1 cm^{-1} and wavefunctions (f better than 0.1%) for $\upsilon \leq 5$ when tested for range and step size in the potential energy curve.

The transition dipole matrix element of eq 1 can be expanded as

$$\langle \upsilon|\vec{\mu}|0\rangle = \frac{\partial \mu}{\partial q}\langle \upsilon|q|0\rangle + \frac{1}{2}\frac{\partial^2 \mu}{\partial q^2}\langle \upsilon|q^2|0\rangle + \frac{1}{6}\frac{\partial^3 \mu}{\partial q^3}\langle \upsilon|q^3|0\rangle + ... \qquad (3)$$

where q is the internal vibrational displacement coordinate. The integrals $\langle \upsilon|q^n|0\rangle$ required for the transition dipole moment are evaluated analytically for the Morse potential[47] and by trapezoidal numeric integration for the numerical potential. The dipole moment coefficients are found from a sixth-order polynomial fit to a nine-point dipole moment curve calculated over values of q from −0.2 to 0.2 Å in 0.05 Å steps.[30,45] These dipole moment coefficients provide oscillator strengths that are converged to better than 1% when compared to larger dipole moment curves.[41,48]

The CCSD(T) dipole moment at each geometry is calculated using a finite field approach with a field strength of ± 0.025 au. The single point threshold criterion was set to energy $= 1 \times 10^{-8}$ au, orbital $= 1 \times 10^{-8}$ au, coefficient $= 1 \times 10^{-8}$ au. All coupled-cluster calculations assume a frozen core (O, 1s; F, 1s; S, 1s, 2s, 2p; Cl, 1s, 2s, 2p). All calculations were performed with MOLPRO.[49]

Results and Discussion

Dissociation Reactions. In Figure 1, we present the CCSD(T)/aug-cc-pV(T+d)Z stationary points for the dissociation of XSO_3H, where X = F, Cl. The reaction pathway for the dissociation reactions is given in Figure 2. For both molecules, the dissociation reaction proceeds via the transition state (TS) and the local minimum ($HX{\cdot}SO_3$). In the transition state, the OH group is rotated so that the hydrogen atom is directed toward the halogen atom. The O−H and S−X bond lengths are

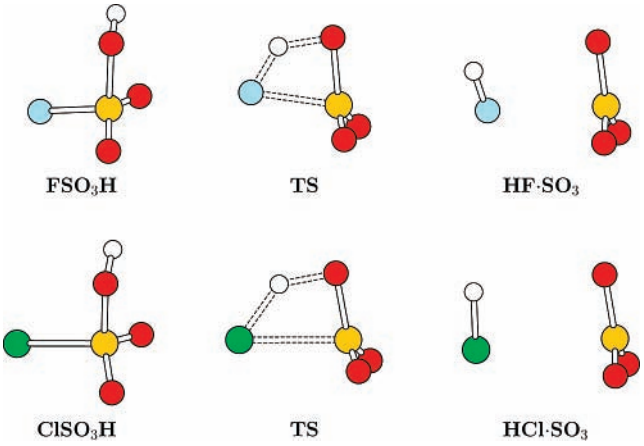

Figure 1. Stationary points for the dissociation of FSO_3H and $ClSO_3H$.

elongated and the H−X distance reduced. The local minima corresponds to the weakly bound HX·SO_3 van der Waals complex.

Reactants. We are not aware of any gas-phase experimental geometries of FSO_3H or $ClSO_3H$ in the literature. However, the geometry of FSO_3H has been previously determined by X-ray diffraction in the solid state at 123 K.[50] With the exception of the O−H bond length, the CCSD(T)/aug-cc-pV(T+d)Z-optimized geometry is in good agreement with the experimentally determined structure. The experimental O−H bond length was found to be unreasonably short at 0.63 Å, which is likely due to the inherent insensitivity of X-ray scattering to hydrogen atoms.[51,52]

In Table 1, we compare selected geometric parameters in XSO_3H calculated with the CCSD(T)/aug-cc-pV(T+d)Z method. We have previously found the CCSD(T)/aug-cc-pV(T+d)Z geometry of H_2SO_4 to be in excellent agreement with the experimental gas-phase geometry determined by microwave spectroscopy.[39,53] In Table 1, we include selected geometric paramters of H_2SO_4 for comparison. Previous low level ab initio and density functional calculations of XSO_3H are in good agreement with our current CCSD(T)/aug-cc-pV(T+d)Z optimized geometries.[51,54] The most obvious difference between FSO_3H and $ClSO_3H$ is the much longer R_{S-X} bond length in $ClSO_3H$, as expected. The effect of the much larger Cl atom, and hence weaker S−X bond, is an elongation of the R_{S-O}, $R_{S=O(1)}$, and $R_{S=O(2)}$ bonds. The fundamental infrared spectrum of XSO_3H and H_2SO_4 support our calculated geometries with the S−O and S=O frequencies of FSO_3H found to be higher than those of $ClSO_3H$ and the frequencies of H_2SO_4 even lower.[55] The orientation of the OH groups in FSO_3H and $ClSO_3H$ are similar with the hydrogen atom in FSO_3H slightly better aligned with the adjacent S=O group. We have previously found that the orientation of the OH group with respect to the adjacent S=O, may allow a weak intramolecular interaction, which can increase the OH bond length and lower the OH-stretching frequency.[39]

Transition State. In Table 2, we present the relative energy between XSO_3H and the TS calculated at the HF, MP2, B3LYP, CCSD, and CCSD(T) levels of theory with the aug-cc-pV(D+d)Z and aug-cc-pV(T+d)Z basis sets. The energies have all been calculated at the optimized geometries of the same method. The relative energies in Table 2 can be thought of as the energy barrier or activation energy required for the dissociation of XSO_3H as illustrated in Figure 2.

The energy required for dissociation of XSO_3H is calculated to be highest at the HF level of theory. The inclusion of electron correlation reduces the energy required for the dissociation of FSO_3H by 14−21 kcal mol^{-1} and for $ClSO_3H$ by 11−18 kcal mol^{-1}. The significant effect of electron correlation reflects its importance in bond-making and bond-breaking processes. We consider the CCSD(T)/aug-cc-pV(T+d)Z results to be the benchmark for comparison to the other methods. We find the MP2 and B3LYP methods slightly underestimate and the CCSD method slightly overestimates the energy required for dissociation. For larger systems, where the CCSD(T) method is not computationally feasible, we suggest that B3LYP/aug-cc-pV(T+d)Z results will be within a few kcal mol^{-1} of CCSD(T)/aug-cc-pV(T+d)Z results. For FSO_3H, the CCSD(T) energy barier increases by 4 kcal mol^{-1} as the basis set increases from aug-cc-pV(D+d)Z to aug-cc-pV(T+d)Z. For $ClSO_3H$, the CCSD(T) energy barrier is less sensitive to basis set with a 2 kcal mol^{-1} increase from aug-cc-pV(D+d)Z to aug-cc-pV(T+d)Z.

In Table 3, we present our best estimate of the energy required for the dissociation of XSO_3H. We give the CCSD(T)/aug-cc-pV(T+d)Z electronic energies and correct for ZPVE with B3LYP/aug-cc-pV(T+d)Z harmonic frequencies. Thermodynamic corrections are also calculated with the B3LYP/aug-cc-pV(T+d)Z method at 298 K. The inclusion of ZPVE and thermodynamic corrections is slightly more significant for $ClSO_3H$ than FSO_3H. ZPVE corrections lower the energy barrier for dissociation of FSO_3H by ~3 kcal mol^{-1} and $ClSO_3H$ by ~4 kcal mol^{-1}. The small difference between the enthalpy barrier (ΔH_{298}) and the Gibbs free energy barrier (ΔG_{298}) is not suprising given both the reactant and transition state consist of single molecule and hence have similar entropy. At 298 K, the Gibbs free energy barrier for the FSO_3H dissociation is 38.2 kcal mol^{-1} (~13 400 cm^{-1}) and for $ClSO_3H$ dissociation it is 29.7 kcal mol^{-1} (~10 400 cm^{-1}). The energy barrier for dissociation of $ClSO_3H$ is likely lower than FSO_3H due to the weaker S−Cl bond, which requires less energy to break as compared to S−F. Hence, dissociation of $ClSO_3H$ should occur with less energy than FSO_3H.

Local Minimum. In Table 4, we present selected geometric parameters for the intermediate HX·SO_3 van der Waals complexes optimized with the CCSD(T)/aug-cc-pV(T+d)Z method. We give both the standard-optimized and CP-optimized geometries as well as the available experimental parameters determined by microwave spectroscopy.[56] The standard-optimized and CP-optimized geometries are very similar, and as expected the most significant difference is the intermolecular distance $R_{S\cdots X}$. BSSE artificially lowers the energy of the complex relative to the monomers; hence, the calculated interaction is too attractive, and the intermolecular distance is underestimated.[38,40] Overall, the CP-optimized geometries of HX·SO_3 are in reasonable agreement with the experimentally determined geometry.[56] In HF·SO_3, the hydrogen atom of HF is directed away from SO_3, while in HCl the hydrogen atom is directed toward the in-plane oxygen atom of SO_3, as seen in Figure 1. Our CCSD(T)/aug-cc-pV(T+d)Z calculated structures are in good agreement with recent MP2/6-311++G(3df,3pd) results.[57] The calculated θ_{S-F-H} angle of HF·SO_3 is in better agreement with the experimental value estimated from the moments of inertia (106°) than the value estimated from the quadruple coupling constants (132°).[56,57] For HCl·SO_3, the calculated value of θ_{S-Cl-H} is ~15° greater than the experimentally determined value.[56] The intermolecular angles of weakly bound complexes generally have very flat potential energy surfaces, which make accurate experimental and calculated geometries difficult to obtain. Furthermore, calculated geometries are obtained at the

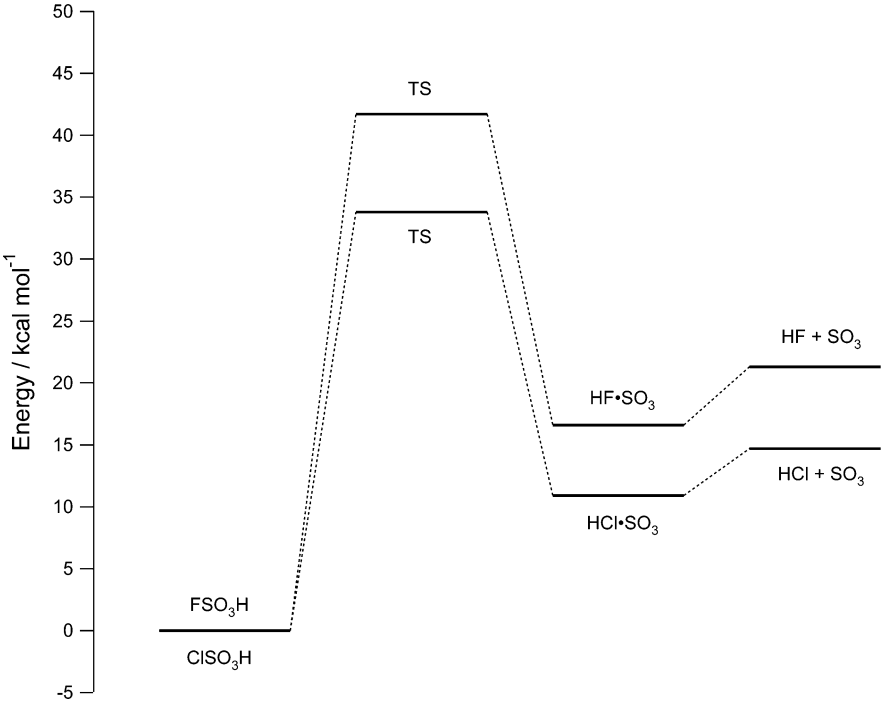

Figure 2. Reaction pathway and energetics for the dissociation of FSO_3H and $ClSO_3H$.

TABLE 1: Selected Geometric Parameters in (Å and degrees) of FSO_3H, $ClSO_3H$, and H_2SO_4[a]

parameter	FSO_3H	$ClSO_3H$	H_2SO_4[b]
R_{O-H}	0.9694	0.9702	0.9687
θ_{H-O-S}	108.8	108.4	108.3
$\phi_{H-O-S-O}$	−23.3	−27.5	−26.3
R_{S-X}	1.5574	2.0301	1.5876
R_{S-O}[c]	1.5722	1.5819	1.5876
$R_{S=O(1)}$[d]	1.4203	1.4262	1.4227
$R_{S=O(2)}$[e]	1.4126	1.4188	1.4227
$R_{X\cdots HO}$	2.7551	3.1015	

[a] Calculated at the CCSD(T)/aug-cc-pV(T+d)Z level of theory. [b] Ref 39. [c] Refers to the S−O bond length of the S−OH group(s). [d] Refers to the O atom closest to the OH group. [e] Refers to the O atom furthest to the OH group

TABLE 2: Electronic Energy Difference (in kcal mol^{-1}) between XSO_3H and the TS

method	FSO_3H	$ClSO_3H$
HF/AV(D+d)Z	55.0	47.0
HF/AV(T+d)Z	59.7	48.1
B3LYP/AV(D+d)Z	35.3	30.3
B3LYP/AV(T+d)Z	38.6	31.2
MP2/AV(D+d)Z	34.5	28.8
MP2/AV(T+d)Z	38.8	31.0
CCSD/AV(D+d)Z	41.0	35.3
CCSD/AV(T+d)Z	45.7	37.6
CCSD(T)/AV(D+d)Z	37.4	31.8
CCSD(T)/AV(T+d)Z	41.7	33.8

TABLE 3: Activation Energy for XSO_3H Dissociation (in kcal mol^{-1})

	FSO_3H	$ClSO_3H$
electronic energy[a]	41.7	33.8
electronic energy+ZPVE[b]	38.3	29.9
ΔH_{298}[c]	38.2	29.8
ΔG_{298}[c]	38.2	29.7

[a] Calculated with the CCSD(T)/aug-cc-pV(T+d)Z method. [b] ZPVE correction calculated with B3LYP/aug-cc-pV(T+d)Z harmonic frequencies. [c] CCSD(T)/aug-cc-pV(T+d)Z electronic energy with a B3LYP/aug-cc-pV(T+d)Z thermodynamic correction at 298 K.

TABLE 4: Selected Geometric Parameters (in Å and Degrees) of $HF\cdot SO_3$ and $HCl\cdot SO_3$[a]

parameter	std opt[b]	CP opt[c]	expt[d]
	$HF\cdot SO_3$		
R_{H-F}	0.924	0.924	0.917
$R_{S\cdots F}$	2.640	2.681	2.655(10)
θ_{S-F-H}	106.8	108.5	106
	$HCl\cdot SO_3$		
R_{H-Cl}	1.279	1.279	1.275
$R_{S\cdots Cl}$	3.094	3.139	3.1328(57)
θ_{S-Cl-H}	87.3	88.2	73

[a] Calculated at the CCSD(T)/aug-cc-pV(T+d)Z level of theory. [b] Calculated using the standard optimization scheme. [c] Calculated using the CP-corrected optimization scheme. [d] From ref 56. Experimental geometry assumes no geometric change in monomers upon complexation.

bottom of the potential energy surface, whereas experimental geometries are measured for the ground vibrational state. Because of the anharmonic nature of the potential, this can give rise to small differences. We have recently found that the intermolecular angles of $H_2O\cdot SO_3$ calculated with the CP-optimized CCSD(T)/aug-cc-pV(T+d)Z method also differ from experiment, perhaps warranting a reanalysis of the experimental geometry.[38,58]

In Table 5, we present the CCSD(T)/aug-cc-pV(T+d)Z calculated binding energies of $HX\cdot SO_3$. The effect of BSSE on the binding energy has been corrected in two different ways. First, a static CP energy correction is made to the standard optimized geometry, denoted "std opt + CP". This is the post priori approach proposed by Boys and Bernardi.[59] Second, the binding energy is calculated using the full CP-optimized geometry, denoted "CP opt". These two counterpoise-corrected binding energies are very similar indicating that for $HX\cdot SO_3$ a simple static CP correction adequately corrects the binding energy for BSSE. This is similar to what we have previously found for the hydrated complexes $H_2O\cdot CO_2$, $H_2O\cdot CS_2$, $H_2O\cdot OCS$, $H_2O\cdot SO_2$, and $H_2O\cdot SO_3$, provided an adequate basis set

TABLE 5: Calculated Binding Energies (in kcal mol^{-1}) for $HX{\cdot}SO_3$

	$HF{\cdot}SO_3$	$HCl{\cdot}SO_3$
std opt	4.7	3.9
std opt + CP[a]	4.0	3.3
CP opt	4.0	3.3
CP opt + ZPVE[b]	3.6	2.9

[a] Static CP correction based on standard CCSD(T)/aug-cc-pV(T+d)Z optimized geometry. [b] ZPVE correction calculated with B3LYP/aug-cc-pV(T+d)Z harmonic frequencies.

TABLE 6: CCSD(T) Calculated OH-Stretching Local Mode Frequencies and Anharmonicities (in cm^{-1}) of FSO_3H, $ClSO_3H$, and H_2SO_4

	aug-cc-pV(D+d)Z		aug-cc-pV(T+d)Z	
basis set	$\tilde{\omega}$	$\tilde{\omega}x$	$\tilde{\omega}$	$\tilde{\omega}x$
FSO_3H	3740.8	85.71	3771.6	79.44
$ClSO_3H$	3732.7	85.96	3759.8	79.60
H_2SO_4[a]	3748.4	85.88	3778.5	79.71

[a] From ref 39.

it used.[38] The inclusion of a ZPVE correction (calculated with harmonic B3LYP/aug-cc-pV(T+d)Z frequencies) lowers the binding energy of $HX{\cdot}SO_3$ by ~0.4 kcal mol^{-1}. Hence, we estimate the binding energy of $HF{\cdot}SO_3$ and $HCl{\cdot}SO_3$ to be 3.6 and 2.9 kcal mol^{-1}, respectively. The binding energies of $HF{\cdot}SO_3$ and $HCl{\cdot}SO_3$ have previously been calculated to be 3.7 and 3.0 kcal mol^{-1}, respectively, with the MP2/6-311++G-(3df,3pd) method.[57] These MP2 values are calculated with a full CP optimization but with no ZPVE correction and hence are, as expected, slightly higher than our present values.

It should be noted that the binding energy of $HF{\cdot}SO_3$ recently calculated by Weber et al. with the B3LYP/6-311++G** method is significantly overestimated at 11.1 kcal mol^{-1}.[28] We have repeated these B3LYP/6-311++G** calculations with both Gaussian 03 and MOLPRO but are unable to reproduce their results.[49,60] We calculate the binding energy of $HF{\cdot}SO_3$ with the B3LYP/6-311++G** method to be 4.2 kcal mol^{-1}, with the inclusion of ZPVE correction lowering the binding energy to 3.2 kcal mol^{-1}. These values are much more reasonable compared with our CCSD(T)/aug-cc-pV(T+d)Z binding energies.

OH-Stretching Transitions. The CCSD(T) calculated local mode parameters for the OH-stretching vibrations of FSO_3H and $ClSO_3H$ are presented in Table 6. For H_2SO_4, the CCSD-(T)/aug-cc-pV(T+d)Z local mode parameters were found to be in good agreement with experiment with $\tilde{\omega}$ overestimated by ~15 cm^{-1} and $\tilde{\omega}x$ calculated within 2 cm^{-1}. The net effect of these discrepancies with experiment was a slight overestimate of the OH-stretching wavenumbers for H_2SO_4. Hence, it is likely that our calculated OH-stretching wavenumbers for FSO_3H and $ClSO_3H$ will also be slightly overestimated.

The frequency $\tilde{\omega}$ of FSO_3H is calculated to be 12 cm^{-1} higher than $ClSO_3H$ with the CCSD(T)/aug-cc-pV(T+d)Z method, whereas the calculated anharmonicities $\tilde{\omega}x$ are very similar. The lower frequency $\tilde{\omega}$ of $ClSO_3H$ is perhaps suprising given the electronegativity of chlorine is less than fluorine. In our previous investigation of the OH-stretching overtone spectra of CH_3SO_3H, H_2SO_4 and CF_3SO_3H, we found the OH-stretching frequency $\tilde{\omega}$ to be inversely proportional to the electronegativity of the subsituent (CH_3 < OH < CF_3).[39] Perhaps a more correct description would have been that the OH-stretching frequency $\tilde{\omega}$ is dependent on the electron donating/withdrawing ability of the substituent with strong electron-withdrawing groups resulting in lower values of $\tilde{\omega}$. The electron-donating/-withdrawing ability of a subsituent depends on both the inductive withdrawal (electronegativity) and resonance donation of electrons.[61] While fluorine is more electronegative than chlorine, it is also better at donating electrons by resonance than chlorine.[61] The higher value of $\tilde{\omega}$ for FSO_3H as compared to $ClSO_3H$ indicates that the effect of electron donation by resonance dominates the effect of inductive withdrawal for halosubstituted sulfonic acid derivatives. This trend is similar to that observed for the well-known electrophilic substitution of a benzene ring.[61]

TABLE 7: OH-Stretching Wavenumbers (in cm^{-1}) and Oscillator Strengths of FSO_3H and $ClSO_3H$ Calculated with Morse Potentials[a]

	FSO_3H		$ClSO_3H$	
v	$\tilde{\nu}$	f	$\tilde{\nu}$	f
1	3613	2.2×10^{-5}	3601	2.2×10^{-5}
2	7067	6.8×10^{-7}	7042	7.1×10^{-7}
3	10362	1.9×10^{-8}	10324	2.0×10^{-8}
4	13498	1.0×10^{-9}	13447	1.1×10^{-9}
5	16475	9.9×10^{-11}	16411	1.0×10^{-10}

[a] Calculated with the CCSD(T)/aug-cc-pV(T+d)Z method.

TABLE 8: OH-Stretching Wavenumbers (in cm^{-1}) and Oscillator Strengths of FSO_3H and $ClSO_3H$ Calculated with Numeric Potentials[a]

	FSO_3H		$ClSO_3H$	
v	$\tilde{\nu}$	f	$\tilde{\nu}$	f
1	3614	2.1×10^{-5}	3602	2.2×10^{-5}
2	7074	7.5×10^{-7}	7049	7.7×10^{-7}
3	10380	2.7×10^{-8}	10343	2.8×10^{-8}
4	13536	1.9×10^{-9}	13486	2.1×10^{-9}
5	16544	2.2×10^{-10}	16480	2.3×10^{-10}

[a] Calculated with the CCSD(T)/aug-cc-pV(T+d)Z method.

In Table 7, we present the wavenumbers and oscillator strengths of the OH-stretching transitions for FSO_3H and $ClSO_3H$ calculated using a Morse potential with local mode parameters and dipole moment functions obtained with CCSD-(T)/aug-cc-pV(T+d)Z method. The fundamental OH-stretching transition of FSO_3H is calculated to be 3613 cm^{-1}, which is 12 cm^{-1} higher than that of $ClSO_3H$ (3601 cm^{-1}). As expected, this difference increases with increasing Δv, up to ~60 cm^{-1} for $\Delta v = 5$. The vapor-phase FT-IR OH-stretching wavenumbers of FSO_3H and $ClSO_3H$ are 3605 and 3587 cm^{-1}, respectively,[55] compared to 3609 cm^{-1} for H_2SO_4.[8] The relative frequencies are in agreement with the relative OH-bond lengths of Table 1.[29]

The higher experimental fundamental wavenumber of FSO_3H compared with $ClSO_3H$ supports our calculated local mode parameters. The agreement between the calculated and experimental fundamental wavenumbers is good. The variation in the calculated oscillator strengths of the OH-stretching transitions in FSO_3H and $ClSO_3H$ is small.

In Table 8 we present the wavenumbers and intensities of the OH-stretching transitions for FSO_3H and $ClSO_3H$ calculated using the numeric solution and a CCSD(T)/aug-cc-pV(T+d)Z potential and dipole moment functions. For the FSO_3H and $ClSO_3H$ fundamental transitions, the wavenumbers calculated with the Morse and numeric potentials are virtually the same. However, the wavenumbers calculated with the two methods diverge for increasing Δv and reach ~70 cm^{-1} at $\Delta v = 5$.

The fundamental OH-stretching oscillator strengths of FSO_3H and $ClSO_3H$ are virtually the same whether calculated with the Morse or numeric potential. For the OH-stretching overtones, the oscillator strengths obtained with the numeric potential are higher than those obtained with the Morse potential. This

difference increases with increasing Δv, by up to a factor of $\sim$2 at $\Delta v = 5$. The large difference in calculated oscillator strengths is due to the difference in the wavefunctions, as the same dipole moment function is used with both methods. This suggests that the Morse potential is an adequate approximation in the lower energy region of the potential, but becomes less suitable to describe the highly vibrationally excited region. We have previously compared oscillator strengths of OH-stretching transitions in water dimer and sulfuric acid obtained with either the Morse or the numeric potentials.[41,48] We find the Morse approach to give consistently lower oscillator strengths than the numeric solution.

Overtone-Induced Photodissociation. We find the dissociation reaction pathway of FSO_3H and $ClSO_3H$ ($XSO_3H \rightarrow HX + SO_3$) to be similar to that of H_2SO_4 ($H_2SO_4 \rightarrow H_2O + SO_3$).[13,14] For FSO_3H, our best estimate of ΔG for the energy barrier for dissociation is 38.2 kcal mol^{-1} ($\sim$13 400 cm^{-1}) at 298 K. This value is based on CCSD(T)/aug-cc-pV(T+d)Z-optimized energies with thermodynamic corrections calculated with the B3LYP/aug-cc-pV(T+d)Z method. For $ClSO_3H$, the energy barrier is calculated to be lower in energy, 29.7 kcal mol^{-1} ($\sim$10 400 cm^{-1}). We find the dissociation energies of FSO_3H and $ClSO_3H$ to be similar to those previously calculated for H_2SO_4 (32$-$40 kcal mol^{-1}) at the MP2 and B3LYP levels of theory.[13,14] From our 1D OH-stretching overtone calculations, we conservatively estimate that excitation of the OH-stretching transitions with $\Delta v \geq 5$ and $\Delta v \geq 4$, will provide adequate energy for photodissociation of FSO_3H and $ClSO_3H$, respectively.

The dissociation of H_2SO_4 in the stratosphere is thought to occur via an OH-stretching overtone-induced mechanism.[3] However, this dissociation mechansim has yet to be confirmed experimentally because of inherent difficulties in monitoring the products of dissociation, H_2O and SO_3. A gas-phase sample of H_2SO_4 suitable for spectroscopic studies is typically produced by mixing known amounts of H_2O and SO_3 vapor at elevated temperatures.[7] However, this approach results in a large background signal from the H_2O and SO_3 starting materials, making it virtually impossible to detect the H_2O and SO_3 as products of OH-stretching overtone-induced photodissociation. FSO_3H and $ClSO_3H$ do not have this problem, and hence experimental detection of HF/HCl and SO_3, products of OH-stretching overtone-induced photodissociation, should be possible without a large background of HF/HCl and SO_3. This perhaps simpler experimental study of FSO_3H and $ClSO_3H$ could be used by proxy to validate the OH-stretching overtone-induced photodissociation mechanism of H_2SO_4.

Conclusions

We have calculated the stationary points and internal reaction pathway for the dissociation of FSO_3H and $ClSO_3H$ to HF + SO_3 and HCl + SO_3, respectively. We have used a range of ab initio and density functional theories with correlation consistent basis sets. We find the energy barrier for dissociation of FSO_3H to be higher than that for $ClSO_3H$. We have calculated the OH-stretching wavenumbers and intensities of FSO_3H and $ClSO_3H$ using the anharmonic oscillator local mode model with local mode parameters and dipole moment functions obtained from CCSD(T) ab initio calculations. We find there to be adequate energy for photodissociation of FSO_3H and $ClSO_3H$ with excitation of the OH-stretching transitions $\Delta v \geq 5$ and $\Delta v \geq 4$, respectively. We propose that experimental detection of the OH-stretching overtone-induced photodissociation of FSO_3H and $ClSO_3H$ could be used by proxy to support the proposed OH-stretching-induced photodissociation mechanism of H_2SO_4 in the stratosphere.

Acknowledgment. We thank Jeppe Olsen for use of his ONEDIM program. We thank Veronica Vaida for helpful discussions. J.R.L is grateful to the Foundation for Research, Science, and Technology for a Bright Futures scholarship. We acknowledge the Lasers and Applications Research Theme at the University of Otago for use of their computer facilities. We acknowledge the Marsden Fund administered by the Royal Society of New Zealand, the Lundbeck Foundation, and the Research Foundation at Aarhus University for financial support.

Supporting Information Available: The optimized electronic energies of the stationary points along the reaction coordinate for dissociation of FSO_3H and $ClSO_3H$ calculated using the HF, MP2, B3LYP, CCSD, and CCSD(T) levels of theory with the aug-cc-pV(D+d)Z and aug-cc-pV(T+d)Z basis sets. The CCSD(T)/AV(D+d)Z and CCSD(T)/AV(T+d)Z geometries for FSO_3H and $ClSO_3H$ in Z-matrix format. This material is available free of charge via the Internet at http://pubs.acs.org.

References and Notes

(1) Charlson, R. J.; Anderson, T. L.; McDuff, R. E. *Earth System Science*; Academic Press: New York, 2000.
(2) Warneck, P. *Chemistry of the Natural Atmosphere*, 2nd ed.; Academic Press: San Diego, CA, 2000.
(3) Vaida, V.; Kjaergaard, H. G.; Hintze, P. E.; Donaldson, D. J. *Science* **2003**, *299*, 1566−1568.
(4) Mills, M. J.; Toon, O. B.; Vaida, V.; Hintze, P. E.; Kjaergaard, H. G.; Schofield, D. P.; Robinson, T. W. *J. Geophys. Res., Atmos*. **2005**, *110*, D08201.
(5) Rosen, J. M.; Hofmann, D. J. *J. Geophys. Res*. **1983**, *88*, 3725−3731.
(6) Hofmann, D. J.; Rosen, J. M. *Geophys. Res. Lett*. **1985**, *12*, 13−16.
(7) Burkholder, J. B.; Mills, M. J.; McKeen, S. *Geophys. Res. Lett*. **2000**, *27*, 2493−2496.
(8) Hintze, P. E.; Kjaergaard, H. G.; Vaida, V.; Burkholder, J. B. *J. Phys. Chem. A* **2003**, *107*, 1112−1118.
(9) Robinson, T. W.; Schofield, D. P.; Kjaergaard, H. G. *J. Chem. Phys.* **2003**, *118*, 7226−7232.
(10) Lane, J. R.; Kjaergaard, H. G. Unpublished.
(11) Crim, F. F. *Ann. Rev. Phys. Chem*. **1984**, *35*, 657−691.
(12) Crim, F. F. *J. Phys. Chem.* **1996**, *100*, 12725−12734.
(13) Morokuma, K.; Muguruma, C. *J. Am. Chem. Soc*. **1994**, *116*, 10316.
(14) Larson, L. J.; Kuno, M.; Tao, F.-M. *J. Chem. Phys.* **2000**, *112*, 8830− 8838.
(15) Hintze, P. E.; Feierabend, K. J.; Havey, D. K.; Vaida, V. *Spectrochim. Acta, Part A* **2005**, *61*, 559−566.
(16) Feierabend, K. J.; Havey, D. K.; Brown, S. S.; Vaida, V. *Chem. Phys. Lett*. **2006**, *420*, 438−442.
(17) Rizzo, T. R.; Hayden, C. C.; Crim, F. F. *Faraday Discuss. Chem. Soc*. **1983**, *75*, 223−237.
(18) Scherer, N. F.; Zewaii, A. H. *J. Chem. Phys*. **1987**, *87*, 97−114.
(19) Ticich, T. M.; Likar, M. D.; Dubal, H. R.; Butler, L. J.; Crim, F. F. *J. Chem. Phys*. **1987**, *87*, 5820−5829.
(20) Sinha, A.; Vander Wal, R. L.; Crim, F. F. *J. Chem. Phys*. **1990**, *92*, 401−410.
(21) Donaldson, D. J.; Tuck, A. F.; Vaida, V. *Phys. Chem. Earth, Part C* **2000**, *25*, 223−227.
(22) Nizkorodov, S. A.; Wennberg, P. O. *J. Phys. Chem. A* **2002**, *106*, 855−859.
(23) Roehl, C. M.; Nizkorodov, S. A.; Zhang, H.; Blake, G. A.; Wennberg, P. O. *J. Phys. Chem. A* **2002**, *106*, 3766−3772.
(24) Konen, I. M.; Pollack, I. B.; Li, E. X. J.; Lester, M. I.; Varner, M. E.; Stanton, J. F. *J. Chem. Phys*. **2005**, *122*, 094320.
(25) Fry, J. L.; Nizkorodov, S. A.; Okumura, M.; Roehl, C. M.; Francisco, J. S.; Wennberg, P. O. *J. Chem. Phys.* **2004**, *121*, 1432−1448.
(26) Fry, J. L.; Matthews, J.; Lane, J. R.; Roehl, C. M.; Sinha, A.; Kjaergaard, H. G.; Wennberg, P. O. *J. Phys. Chem. A* **2006**, *110*, 7072−7079.
(27) Staikova, M.; Oh, M.; Donaldson, D. J. *J. Phys. Chem. A* **2005**, *109*, 597−602.
(28) Weber, K. H.; Harris, J. A.; Larson, L. J.; Tao, F.-M.; Li, S.; Gu, R. *J. Theor. Comput. Chem*. **2005**, *4*, 623−638.
(29) Henry, B. R. *Acc. Chem. Res*. **1977**, *10*, 207−213.

(30) Kjaergaard, H. G.; Henry, B. R. *J. Chem. Phys.* **1992**, *96*, 4841−4851.
(31) Tarr, A. W.; Zerbetto, F. *Chem. Phys. Lett.* **1989**, *154*, 273−279.
(32) Donaldson, D. J.; Orlando, J. J.; Amann, S.; Tyndall, G. S.; Proos, R. J.; Henry, B. R.; Vaida, V. *J. Phys. Chem. A* **1998**, *102*, 5171−5174.
(33) Kjaergaard, H. G. *J. Phys. Chem. A* **2002**, *106*, 2979−2987.
(34) Henry, B. R.; Kjaergaard, H. G. *Can. J. Chem.* **2002**, *80*, 1635−1642.
(35) Howard, D. L.; Jørgensen, P.; Kjaergaard, H. G. *J. Am. Chem. Soc.* **2005**, *127*, 17096−17103.
(36) Wilson, A. K.; Peterson, K. A.; Dunning, T. H. *J. Chem. Phys.* **2001**, *114*, 9244−9253.
(37) Wilson, A. K.; Dunning, T. H., Jr. *J. Chem. Phys.* **2003**, *119*, 11712−11714.
(38) Garden, A. L.; Lane, J. R.; Kjaergaard, H. G. *J. Chem. Phys.* **2006**, *125*, 144317.
(39) Lane, J. R.; Kjaergaard, H. G.; Plath, K. P.; Vaida, V. *J. Phys. Chem. A* **2007**, *111*, 5434−5440.
(40) Simon, S.; Duran, M.; Dannenberg, J. J. *J. Chem. Phys.* **1996**, *105*, 11024−11031.
(41) Schofield, D. P.; Lane, J. R.; Kjaergaard, H. G. *J. Phys. Chem A* **2007**, *111*, 567−572.
(42) Atkins, P. W.; Friedman, R. S. *Molecular Quantum Mechanics*, 3rd ed.; Oxford University Press: Oxford, 1997.
(43) Kjaergaard, H. G.; Yu, H.; Schattka, B. J.; Henry, B. R.; Tarr, A. W. *J. Chem. Phys.* **1990**, *93*, 6239−6248.
(44) Herzberg, G. *Molecular Spectra and Molecular Structure I. Spectra of Diatomic Molecules*; D. Van Nostrand Company, Inc.: Princeton, NJ, 1950**.**
(45) Low, G. R.; Kjaergaard, H. G. *J. Chem. Phys.* **1999**, *110*, 9104−9115.
(46) Onedim program. Olsen, J. Private Communication.
(47) Rong, Z.; Cavagnat, D.; Lespade, L. In *Lecture Notes in Computer Science*; Sloot, P., Ed.; Springer-Verlay: Berlin, 2003; Vol. 2658, p 350−356.
(48) Kjaergaard, H. G.; Garden, A. L.; Lane, J. R.; Robinson, T. W.; Schofield, D. P.; Mills, M. J. *Adv. Quantum Chem.*, in press.
(49) Werner, H.-J.; Knowles, P. J.; Lindh, R.; Manby, F. R.; Schütz, M.; Celani, P.; Korona, T.; Rauhut, G.; Amos, R. D.; Bernhardsson, A.; Berning, A.; Cooper, D. L.; Deegan, M. J. O.; Dobbyn, A. J.; Eckert, F.; Hampel, C.; Hetzer, G.; Lloyd, A. W.; McNicholas, S. J.; Meyer, W.; Mura, M. E.; Nicklass, A.; Palmieri, P.; Pitzer, R.; Schumann, U.; Stoll, H.; Stone, A. J.; Tarroni, R.; Thorsteinsson, T. *Molpro*, version 2006.1; Cardiff, UK, 2006.
(50) Bartmann, K.; Mootz, D. *Acta. Crystallogr., Sect. C* **1990**, *46*, 319−320.
(51) Varetti, E. L. *J. Mol. Struc.* **1998**, *429*, 121−130.
(52) McLain, S. E.; Benmore, C. J.; Turner, J. F. C. *J. Chem. Phys.* **2002**, *117*, 3816−3821.
(53) Kuczkowski, R. L.; Suenram, R. D.; Lovas, F. J. *J. Am. Chem. Soc.* **1981**, *103*, 2561−2566.
(54) Badawi, H. M. *Spectrochim. Acta, Part A* **2007**, *66*, 194−198.
(55) Chackalackal, S. M.; Stafford, F. E. *J. Am. Chem. Soc.* **1966**, *88*, 4815−4819.
(56) Canagaratna, M.; Phillips, J. A.; Goodfriend, H.; Fiacco, D. L.; Ott, M. E.; Harms, B.; Leopold, K. R. *J. Mol. Spec.* **1998**, *192*, 338−347.
(57) Choo, J.; Kim, S.; Kwon, Y. *Chem. Phys. Lett.* **2002**, *358*, 121−129.
(58) Phillips, J. A.; Canagaratna, M.; Goodfriend, H.; Leopold, K. R. *J. Phys. Chem.* **1995**, *99*, 501.
(59) Boys, S. F.; Bernardi, F. *Mol. Phys.* **1970**, *19*, 553−566.
(60) Frisch, M. J.; Trucks, G. W.; Schlegel, H. B.; Scuseria, G. E.; Robb, M. A.; Cheeseman, J. R.; Montgomery, J. A., Jr.; Vreven, T.; Kudin, K. N.; Burant, J. C.; Millam, J. M.; Iyengar, S. S.; Tomasi, J.; Barone, V.; Mennucci, B.; Cossi, M.; Scalmani, G.; Rega, N.; Petersson, G. A.; Nakatsuji, H.; Hada, M.; Ehara, M.; Toyota, K.; Fukuda, R.; Hasegawa, J.; Ishida, M.; Nakajima, T.; Honda, Y.; Kitao, O.; Nakai, H.; Klene, M.; Li, X.; Knox, J. E.; Hratchian, H. P.; Cross, J. B.; Adamo, C.; Jaramillo, J.; Gomperts, R.; Stratmann, R. E.; Yazyev, O.; Austin, A. J.; Cammi, R.; Pomelli, C.; Ochterski, J. W.; Ayala, P. Y.; Morokuma, K.; Voth, G. A.; Salvador, P.; Dannenberg, J. J.; Zakrzewski, V. G.; Dapprich, S.; Daniels, A. D.; Strain, M. C.; Farkas, O.; Malick, D. K.; Rabuck, A. D.; Raghavachari, K.; Foresman, J. B.; Ortiz, J. V.; Cui, Q.; Baboul, A. G.; Clifford, S.; Cioslowski, J.; Stefanov, B. B.; Liu, G.; Liashenko, A.; Piskorz, P.; Komaromi, I.; Martin, R. L.; Fox, D. J.; Keith, T.; Al-Laham, M. A.; Peng, C. Y.; Nanayakkara, A.; Challacombe, M.; Gill, P. M. W.; Johnson, B.; Chen, W.; Wong, M. W.; Gonzalez, C.; Pople, J. A. *Gaussian 03*, revision C.02; Gaussian, Inc.: Wallingford, CT, 2004.
(61) Bruice, P. Y. *Organic Chemistry*; Prentice Hall: New York, 1995.